PHYSICAL REVIEW E **71**, 040801(R) (2005)

Density profiles of temperature-sensitive microgel particles

T. G. Mason[1,*] and M. Y. Lin[2]

[1]*Department of Chemistry and Biochemistry, and Department of Physics and Astronomy, University of California, Los Angeles, 607 Charles E. Young Drive East, Los Angeles, California 90095 USA*

[2]*Center for Neutron Research, National Institute of Standards and Technology, Gaithersburg, Maryland 20899 USA*

(Received 8 November 2004; published 18 April 2005)

We have performed small angle neutron scattering measurements (SANS) on dilute aqueous dispersions of polymer microgel particles as a function of temperature, T. The microgel particles are spherical crosslinked assemblies of a loose gel network of a poly-N-isopropylacrylamide (NIPAM) polymer. When the temperature is raised beyond a critical temperature, $T_{lc} \approx 32\ ^\circ\mathrm{C}$, the polymer becomes more strongly attracted to itself than the solvent, and the microgel particles contract. The measured form factor, $F(q)$, for dilute suspensions of uniform microgel particles exhibits many peaks that are characteristic of solid polymer nanospheres. The position and amplitude of the peaks as a function of wave number, q, provide insight into the density profile of poly-NIPAM within the microgels. These peaks can be described well over a wide range of temperature by a model of the polymer density within the particles that is constant up to an inner radius, R_1, and decreases linearly to zero at an outer radius, R_2.

DOI: 10.1103/PhysRevE.71.040801 PACS number(s): 61.41.+e, 61.12.−q, 61.46.+w, 83.80.Kn

Common polymer "latex" microspheres are made by a variety of processes, including emulsion polymerization [1,2] that yield a uniform dispersion of dense and solid polymer balls in a liquid phase. These microspheres are common in many applications ranging from paints to biomarkers in cells, and the particles may or may not contain an additional crosslinking species to provide additional mechanical stability. By contrast, microgels are dispersions of micron-sized spherical porous gels of a crosslinked polymer [3]. Due to their porous internal polymer network, microgels have interesting physical properties that are not seen with common microspheres. Perhaps the most important of these is the ability to tune the size of the microgel particles by changing the relative attractions of the polymer to itself and to the liquid solvent through the temperature, T. Precipitation polymerization methods have been developed to synthesize uniform aqueous dispersions of microgels, and the most common are comprised of poly-N-isopropylacrylamide (poly-NIPAM), which has a lower critical solution temperature (LCST), $T_{lc} \approx 32\ ^\circ\mathrm{C}$, cross-linked with a small fraction of methylene-bis-acrylamide (BA) [3]. The cross-linker is essential for preventing the microgel particles from simply dissolving and dispersing in the water. Typically, the poly-NIPAM is negatively charged, leading to charge stabilization of the microgels against aggregation.

The phase behavior, structure, and rheology of microgel dispersions can be highly sensitive to changes in temperature around T_{lc}. In concentrated solutions of microgels, the effective volume fraction can be controlled both through the temperature and through the ionic strength that screens the charge interactions between the particles. Dynamic light scattering [4,5] and pulsed field gradient NMR [6] have been used to study the structural relaxation and glass transition in dense microgel suspensions. Colloidal crystals of microgel particles can also be made [7], and the phase behavior of microgel colloids has been investigated experimentally [8] and theoretically [9]. Rheological studies [10–13] have shown that decreasing the temperature of concentrated microgel dispersions from above to below T_{lc} can lead to a dramatic increase in their steady shear viscosity and linear elastic modulus. Small angle neutron scattering (SANS) measurements of microgels [5,14–16] have recently begun to address the issue of the polymer density inside the particles. Due to polydispersity in the size distribution of the microgel particles and due to the limitations of the resolution and accessible angular range of the neutron scattering apparatus, no clear measurements of the form factor have been made as a function of temperature that show many orders of shoulders or peaks that one would expect from interference effects arising from monodisperse spherical particles. At most, one or perhaps two shoulders have been observed. The lack of strong interference effects in the observed neutron scattering intensities has hindered the direct interpretation of the internal structure of the microgels as a function of temperature using a simple model.

Here we present SANS measurements of highly monodisperse anionic poly-NIPAM microgels at a dilute concentration that clearly reveal the particulate nature of these dispersions through peaks in the form factor, $F(q)$, up to the seventh order. Our measurements cover a range of temperatures above and below T_{lc}, and, through the changes in the amplitude and position of the peaks in the wave number q, we are able to discern how temperature changes affect the average size and internal structure of the microgels. We fit these measurements with a simple, yet powerful, description of the form factor of the microgels that is based on a model of the polymer density within the particles that is constant out to a radius, R_1, and decreases linearly down to zero at a larger radius, R_2. This simple model enables us to fit the peaks in the measured form factor accurately over a wide range of temperatures, thereby providing a measurement of the average polymer density profile within the microgels *in situ* above and below the transition temperature.

*Author to whom correspondence should be addressed.

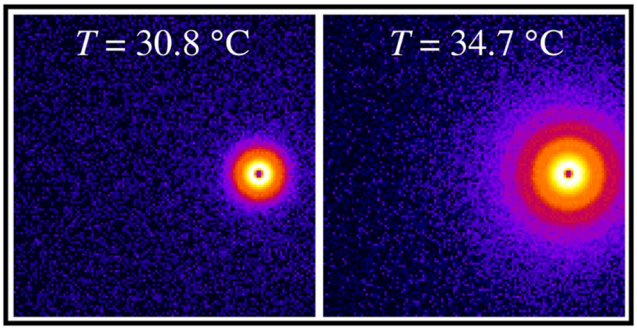

FIG. 1. (Color online) False color images of the small angle neutron scattering patterns from poly-NIPAM microgel particles at 1% by mass in a 9:1 mixture of $D_2O:H_2O$. Temperatures are: $T=30.8\ ^\circ C < T_{lc}$ (left) and $T=34.7\ ^\circ C > T_{lc}$ (right). The brighter and darker colors correspond to higher and lower intensities, respectively. The transmitted beam has been blocked (small dark inner circle), and the detector has been shifted out of the center to provide a greater range of scattering angles. Bright concentric rings around the beam block are observed to shift toward larger scattering angles as the temperature is increased.

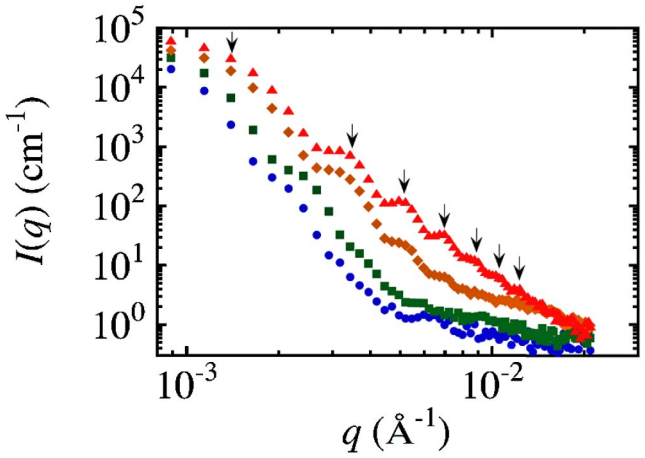

FIG. 2. (Color online) Azimuthally averaged scattering intensity, I, as a function of wave number, q, of dilute microgels described in Fig. 1 for the following temperatures: $T=24.6$ (circles), 30.8 (squares), 32.6 (diamonds), and 34.7 °C (triangles). The scattering intensity decreases rapidly with q at lower temperatures. At the highest temperature, seven peaks or shoulders are clearly visible (arrows).

In order to increase the neutron scattering contrast and reduce the incoherent scattering, we have diluted uniform poly-NIPAM microgel particles (Interfacial Dynamics Corporation) at a mass fraction of $\phi_m=0.1$ solids in H_2O with nine parts of deionized D_2O to obtain a dispersion of $\phi_m=0.01$ in an aqueous continuous phase containing 90% D_2O. The microgel particles have 2.5% BA cross-linker relative to poly-NIPAM by mass and a very low coefficient of variation in diameter of 5%, determined using transmission electron microscopy. After loading this dilute dispersion into a quartz banjo cell of 1 mm path length, we measure the scattering intensity, $I(q)$ as a function of temperature: $T=24.6$, 30.8, 32.6, and 34.7 °C. We start at low temperature and step the temperature up, permitting the sample to equilibrate at the new temperature over a time of 10 min before commencing the next measurement. We use the lowest q range available on the NG-7 beamline at NIST's Center for Neutron Research at an operating wavelength of $\lambda=8$ Å: $0.0008\ \text{Å}^{-1} \leqslant q \leqslant 0.03\ \text{Å}^{-1}$. This configuration enables us to view the relevant q range for our particular dispersion with the best resolution of the details in the scattered intensity.

The two-dimensional scattering patterns from the array detector are shown in false color in Fig. 1 for temperatures below and above T_{lc}. Below T_{lc}, most of the scattering is concentrated at low q, and several concentric rings are visible. At the highest temperature, above T_{lc}, the scattering becomes stronger at higher q and more rings are visible. The azimuthally averaged scattering intensities, $I(q)=F(q)$, for the dilute microgel dispersion are shown as a function of temperature in Fig. 2. At low temperature, the intensity drops off swiftly, even at the lowest q we can access, and several shoulders are visible before the coherent scattering reaches the incoherent scattering background. As the temperature is raised, the intensity increases, the shoulders become more distinct, grow in number, and move toward higher q. At the highest temperatures, the shoulders at the lowest q can actually be distinguished as peaks, and we are able to see up to seven orders extending out toward the highest q in our measurement window. These peaks correspond to the concentric rings in Fig. 1. We have investigated temperatures down to 20 and up to 44 °C, and there is no appreciable change in $I(q)$ from that which we present at 24.6 and 34.7 °C, respectively.

Our scattering measurement is equivalent to measuring the Fourier transform of the density of scattering sites within the microgel particle, ensemble averaged over the distribution of density profiles (i.e., size distribution) of microgel particles [17,18]. The positions of the peaks are a primary indicator of the interference effects resulting from coherent scattering from the most common particles in the sample. The depth of the minima around the peaks is an indication of the polydispersity of the density profiles: more visible minima correspond to a higher degree of uniformity of the density profile among the particles in the sample. In general, the direct inversion of the scattering data into real-space information about the density profile is an ill-posed problem mathematically. Alternatively, one may assume a functional form for the density profile, calculate the form factor, and determine if it matches the data well or not by fitting the data. Although this procedure can often provide satisfying results, there is no guarantee of the uniqueness of the solution for the assumed density profile. However, one may have more confidence in the validity of this method if the fitting parameters make physical sense. In our case, with microgels, the temperature dependence of the fitting parameters would have to make sense with the known contraction (i.e., shrinking) of the particles at higher temperatures above T_{lc}.

We have attempted to fit the shoulders and peaks in Fig. 2 using a form factor corresponding to a simple solid core of constant density out to a radius, R, which can be used to accurately describe solid latex microspheres [17]. This model is not able to capture the positions and amplitudes of all of the peaks and shoulders in Fig. 2 correctly even at the high-

est temperatures we probe, where the microgels are most compact. Moreover, this uniform sphere model cannot capture the more rapid decrease in the measured $F(q)$ at the lower temperatures. Since the peaks and minima of this form factor are primarily a result of interference effects, the addition of polydispersity of particle sizes to the fits does not improve the comparison with the measurements significantly. Although the fits are not satisfactory at any temperature, there is better agreement of this model at higher temperatures where the particles are more compact.

In order to improve the fits, we have calculated the form factor for a particle that has a spherically symmetric density as a function of radius, $\rho(r)$, that is constant in the "core" out to an inner radius, R_1, beyond which the density decreases linearly to zero at an outer radius, R_2. To do so, we square the integral of $\rho(r)[\sin(qr)/(qr)]$ over all space and normalize this by the square of the integral of $\rho(r)$ over all space. The resulting form factor for this "uniform core-linear shell" (UCLS) model is

$$F_{\mathrm{UCLS}}(q) = \frac{144[2\cos(qR_1) - 2\cos(qR_2) + qR_1\sin(qR_1) - qR_2\sin(qR_2)]^2}{[(qR_2)^4 - (qR_1)^4]^2}. \quad (1)$$

Unlike the simple uniform core model, due to the linearly decreasing shell, the UCLS model can produce peaks in the form factor that decay more rapidly than q^{-4}, the power law associated with the decrease in peaks for the uniform core model. This is critical for capturing the strong decay in the peaks of the measured $F(q)$ that is more rapid than q^{-4} at the lower temperatures. Moreover, the UCLS model is easier to implement in a fitting routine than the finely stratified sphere model [19], which has been used to describe the form factor of homogeneous spheres covered by a film with an arbitrary variable refractive index. Given the finite size of the microgel particles, the UCLS model is more realistic physically than an exponential decay proposed for the dielectric permittivity in light scattering results [20], since the UCLS model imposes $\rho(r)=0$ for $r \geqslant R_2$.

We fit the measured data to the UCLS model given and also include a constant background scattering term, I_{incoh}, to account for the incoherent scattering at high q. The total fitting form for the measured $I(q)$ is

$$I(q) = I_0 F_{\mathrm{UCLS}}(q) + I_{\mathrm{incoh}}, \quad (2)$$

where I_0 accounts for the scattering contrast between the polymer and the solvent. The results are shown in Fig. 3. We are able to quantitatively capture the peak positions and amplitudes accurately with this single formula; however, the smeared intensity between the peaks is not described well by the sharp minima of the fitting form, which does not account for polydispersity in the density profile distribution of the microgels. It is remarkable that a single fitting form with only one additional parameter is able to capture the essential features of the data at temperatures both below and above the lower solution critical temperature. We have also tested a model that has a quadratic decrease in density beyond a solid shell, and this model cannot reproduce the peak positions and amplitudes as accurately. Similarly, a solid core-constant shell model, which introduces two additional fitting parameters, does not significantly improve the quality of the fits.

We show the variation of the size fitting parameters R_1 and R_2 as a function of temperature in Fig. 4. Since R_1 remains relatively constant around 170 nm, within the errors, the core itself does not change much in size as a function of temperature; on average, it is perhaps a bit smaller at temperatures below T_{lc}. However, R_2 decreases sharply from about 325 nm for $T < T_{\mathrm{lc}}$ to about 180 nm for $T > T_{\mathrm{lc}}$. This accounts for the known compaction of the particles at temperatures above T_{lc}. This would suggest that most of the reduction in the effective size of the microgel particles at higher temperatures is due to the compaction of a relatively diffuse gradient layer that is on the outside of a uniform core that remains largely unchanged. For these different fits, I_{incoh} and I_0 are essentially independent of T: $I_{\mathrm{incoh}} \approx 1\ \mathrm{cm}^{-1}$ and $I_0 \approx 10^5\ \mathrm{cm}^{-1}$.

This study of the polymer density profiles within microgel particles as a function of temperature clearly reveals the

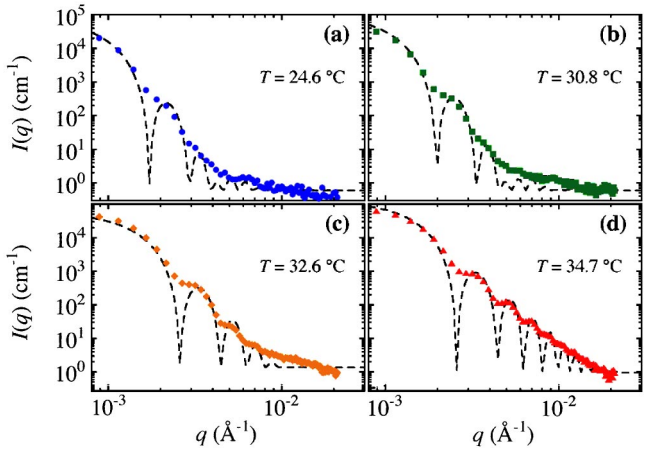

FIG. 3. (Color online) Fits (dashed lines) to the measured scattering intensity, $I(q)$, using the uniform core-linear shell (UCLS) model given in Eqs. (1) and (2) for the following temperatures, T: (a) 24.6 °C (circles), (b) 30.8 °C (squares), (c) 32.6 °C (diamonds), and (d) 34.7 °C (triangles). A single model with two adjustable size parameters can account for the amplitude and position of the observed peaks over a range of temperatures. The sharp minima of the model are not observed due to polydispersity in the microgel density profiles and therefore R_1 and R_2.

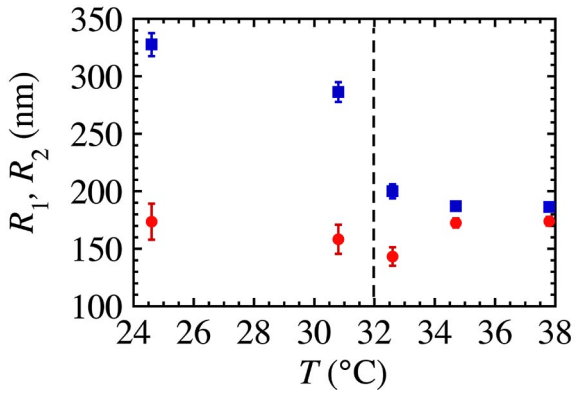

FIG. 4. (Color online) Variation of the fitting parameters for the inner radius, R_1 (circles), and outer radius, R_2 (squares), with temperature, T, obtained from the fits to the UCLS model in Fig. 3 (error bars indicate standard deviations in the fitting parameters). The inner radius remains relatively constant, whereas the outer radius decreases sharply above the lower critical solution temperature, $T_{lc} \approx 32$ °C, for poly-NIPAM (dashed line).

strong interference effects in the form factor arising from the particulate nature of the microgels. Previous SANS studies of microgels have not combined the high density of data points at lower q with the high degree of size monodispersity that would clearly reveal so many peaks in the form factor. We have shown that the relatively simple UCLS model for the density profile of the microgels is sufficient to fit the amplitudes and positions of the peaks in the form factor. Moreover, the temperature dependence of R_2 corresponds well with changes in the hydrodynamic radius that have been measured using dynamic light scattering (DLS) [3,5,14,21]; for 2.5% cross-linker density, we obtain a reduction in $R_2(T)$ that is consistent with previous DLS measurements [21]. To obtain even better fits that can account for the smeared intensity between the observed peaks, it is possible to assume a functional form for the distribution of radii R_1 and R_2 and to numerically perform a least-squares fit in order to optimize the width and skew of the distributions. This analytical approach lies beyond the scope of this paper, and it leads only to refinements of the main points that we have presented. Ultimately, a theoretical description of the origin of the density profiles of microgel particles that accounts for the charge density, cross-linking density, and relative polymer-polymer and polymer-solvent interactions is needed.

We thank NIST's Center for Neutron Research for the NG7 SANS beam time, and Dr. Jim Goodwin for providing the highly monodisperse microgel particles. We thank Dr. John McTague for financially supporting this work through the McTague Chair at UCLA. We have enjoyed stimulating discussions with Dr. Barbara Frisken.

[1] J. Ugelstad, F. K. Hansen, and S. Lange, Makromol. Chem. **175**, 507 (1974).
[2] P. L. Tang *et al.*, J. Appl. Polym. Sci. **43**, 1059 (1991).
[3] R. Pelton, Adv. Colloid Interface Sci. **85**, 1 (2000).
[4] E. Bartsch *et al.*, J. Chem. Phys. **97**, 3950 (1992).
[5] A. Fernández-Barbero *et al.*, Phys. Rev. E **66**, 051803 (2002).
[6] G. Fleischer, H. Hillescu, and V. D. Skirda, Polymer **35**, 1936 (1994).
[7] T. Hellweg *et al.*, Colloid Polym. Sci. **278**, 972 (2000).
[8] J. Wu, B. Zhou, and Z. Hu, Phys. Rev. Lett. **90**, 048304 (2003).
[9] D. Gottwald *et al.*, Phys. Rev. Lett. **92**, 068301 (2004).
[10] R. J. J. Ketz, R. K. Prud'homme, and W. W. Graessley, Rheol. Acta **27**, 531 (1988).
[11] D. M. Öle Kiminta, P. F. Luckham, and S. Lenon, Polymer **36**, 4827 (1995).
[12] J. W. Goodwin and T. J. Huang, in *Modern Aspects of Colloidal Dispersions*, edited by R. H. Ottewill and A. R. Rennie (Kluwer, Dordrecht, 1998), p. 25.
[13] B. H. Tan *et al.*, Polymer **45**, 5515 (2004).
[14] B. R. Saunders, Langmuir **20**, 3925 (2004).
[15] M. Stieger *et al.*, J. Chem. Phys. **120**, 6197 (2004).
[16] M. Stieger, P. Lindner, and W. Richtering, J. Phys.: Condens. Matter **16**, S3861 (2004).
[17] C. S. J. Johnson and D. A. Gabriel, *Laser Light Scattering* (Dover, New York, 1981).
[18] P. M. Chaikin and T. Lubensky, *Principles of Condensed Matter Physics* (Cambridge University Press, Cambridge, 1995).
[19] L. Kai, Z. Min, and A. D'Alessio, J. Mod. Opt. **42**, 507 (1995).
[20] A. Fernández-Nieves, F. J. de las Nieves, and A. Fernández-Barbero, J. Chem. Phys. **120**, 374 (2004).
[21] I. Varga *et al.*, J. Phys. Chem. B **105**, 9071 (2001).